SIAM J. APPL. MATH.
Vol. 47, No. 2, April 1987

006

ON SOME ASPECTS OF THE TRANSONIC CONTROVERSY*

YUE-KUEN KWOK†‡ AND LAWRENCE SIROVICH†

Abstract. The flow of an inviscid, irrotational and compressible perfect gas in the upper half plane is used as a basis for consideration of the transonic controversy. The solution of the complete potential equation for the velocity potential $\phi(x, y)$, with boundary condition $\phi + c\phi_y = U \sin x$ on $y = 0$, is developed as a regular perturbation series. Thirty-six terms of the series are determined by computer. The effective boundary condition is varied with the choice of c; for each of the velocity series, its nature and the location of the singularity nearest to the origin are investigated using the ratio method of Domb and Sykes, and Padé approximants. The result of the analysis shows that the phenomenon of shockless transonic flow is dependent on the imposed boundary condition, which for this example is mediated by the constant c. The relationship of series convergence to local sonic conditions shows no obvious pattern. Cases for which convergence lies below, above or is at criticality were found. Moreover, the connection of divergence to the appearance of shocks is also not apparent. For one class of flows divergent series could be resummed to yield shockless conditions for all Mach numbers. For certain values of c no physically acceptable flow exists.

Key words. transonic flow, potential flow, computer-extended series

AMS(MOS) subject classification. 76G15

PACS number. 47.40.Hg

1. Introduction. Since the 1940's there has been a controversy [1]-[3] over the appearance of shock waves whenever the critical Mach number is exceeded. The well-known Morawetz theorem [4] demonstrates that smooth, i.e., shockless, flows with embedded supersonic regions are mathematically isolated. Any perturbation of the airfoil surface embedded in the supersonic region would cause the commencement of a shock in the flow field. Recently, Van Dyke and Guttmann [5] computed 29 terms of the M^2-series expansion for inviscid, irrotational compressible flow past a circular cylinder. From the power series for the maximum velocity obtained, they found that the estimate of the radius of convergence of the series was higher than the estimate of the critical Mach number by some 1.1%. They concluded that the circular airfoil can have a continuous range of smooth, shock-free potential flows above the critical Mach number.

Along these same lines we note that it is common in the literature to find that breakdown in convergence is taken to imply the nonexistence of smooth solutions—and hence the appearance of shocks in the physical flow. This conclusion has not been proved, and at least for one set of cases we show that it is untrue. In § 3 we exhibit a class of problems for which breakdown occurs because of an *unphysical* singularity in the complex plane. After a routine mapping of this singularity to infinity, smooth solutions are found for all Mach numbers.

Compressible flow over a wavy wall has been used on several occasions to investigate the transonic controversy. The earliest work, by Görtler [6], dates back to 1940. He calculated terms up to third order using the Hantzsche-Wendt method [3] for compressible flow past a kind of wavy wall. To reduce the algebra of computation, he adopted the simple boundary condition for the disturbance potential ϕ to be

$$\phi = K \cos(2\pi x/l) \quad \text{on } y = 0, \tag{1.1}$$

* Received by the editors December 20, 1985; accepted for publication April 3, 1986. This work was supported by the Air Force Office of Scientific Research under grant AFOSR-83-0336.

† Division of Applied Mathematics, Brown University, Providence, Rhode Island 02912.

‡ Present address, Department of Mathematics, West Virginia University, Morgantown, West Virginia 26506.

which is approximately a solid wall of wavelength l centered at $y=0$. He found a continuous supercritical flow with local supersonic regions. The solution was also attempted with the alternative boundary condition, $\partial\phi/\partial y = K\cos(2\pi x/l)$ on $y=0$. This however did not lead to smooth solutions. For the case of an exactly sinusoidal wall, the perturbation series solution of Imai and Oyama [7] using the thin-wing expansion method seems to be divergent above the critical Mach number. In works by Kaplan [8], [9] the perturbation series for the velocity potential, computed using the transonic small perturbation equation, is also found to diverge above the critical Mach number. More recently, Bollmann [10] extended the perturbation series of Kaplan, to 40 terms, using a computer and his analysis of the series led to the same conclusion.

The present study may be regarded as an extension of the approach of Görtler. We consider steady, inviscid, irrotational compressible flow in the upper half plane ($y \geqq 0$) with the boundary condition

$$\phi + c\phi_y = U\sin x \quad \text{on } y=0, \tag{1.2a}$$

$$\phi \to 0 \quad \text{as } y \to \infty \tag{1.2b}$$

where $\phi = \phi(x, y)$ is the velocity potential and c is a parameter which is varied. Although (1.2a) is unusual for gas dynamics it is not in the context of heat flow in which it appears in the Robin problem [11].

Note that there is no uniform upstream flow in this formulation. However, it can be assumed that a blowing and suction mechanism along $y=0$ occurs so that the desired flow field is obtained and satisfies the above boundary conditions.

The rationale behind constructing such flows is to reduce the algebra in computing the perturbation series. Since there is no upstream flow in the problem, the perturbation parameter will not be the free stream Mach number as is usually the case for the Jansen-Rayleigh expansion. Indeed, from energy conservation, we have

$$\frac{q^2}{2} + \frac{a^2}{(\gamma-1)} = \frac{Q^2}{2} \tag{1.3}$$

where $q^2 = \nabla\phi \cdot \nabla\phi$ is the square of local speed, a is the acoustic speed, γ is the ratio of specific heats and Q^2 constant. The natural perturbation parameter in the problem will be

$$\delta = U^2/Q^2 \tag{1.4}$$

where U is defined in the boundary condition (1.2a).

The boundary condition imposed along $y=0$ varies with different values of the parameter c (see 1.2a). With each such boundary condition, the perturbation series for the velocity is developed up to 36 terms. Then the location and nature of the singularity nearest to the origin of each of the series are investigated using Domb and Sykes' ratio method [12], [13] and Padé approximants [14]-[20]. The radius of convergence of the series is compared with the value δ_{cr} at which local sonic speed is first attained.

This present work may be regarded as a regular perturbation problem. Unlike the classical approach of calculating the higher order terms of the perturbation series analytically, the routine labour is delegated to a computer. This work contributes another example to the subject of extending perturbation series by a computer in fluid mechanics. Excellent reviews of this subject have been given by Van Dyke [21]-[23].

2. Series derivation. Consider steady, two-dimensional flow of an inviscid, irrotational, compressible perfect gas in the upper half plane ($y \geqq 0$). The nonlinear second order partial differential equation for compressible potential flow is given by

(2.1) $$a^2\nabla^2\phi = \nabla\phi \cdot \nabla(q^2/2).$$

From energy conservation, we have the Bernoulli relation, given by (1.3). In numerical calculations γ will be taken to be 1.4. If (1.3) is substituted into (2.1) we obtain

(2.2) $$\nabla^2\phi = (q^2/Q^2)\nabla^2\phi + [1/(\gamma-1)]\nabla\phi \cdot \nabla(q^2/Q^2).$$

Henceforth we normalize both the velocity potential ϕ and the velocity q by U. Then (2.2) can be rewritten as

(2.3) $$\nabla^2\phi = \delta q^2\nabla^2\phi + [1/(\gamma-1)]\delta\nabla\phi \cdot \nabla q^2$$

where δ is defined in (1.4).

We adopt a regular perturbation expansion and assume that the velocity potential ϕ can be expanded in the form

(2.4) $$\phi = \phi_0 + \delta\phi_1 + \delta^2\phi_2 + \cdots.$$

Notice that the right-hand side of (2.3) involves triple products in ϕ. The computational complexity can be reduced by treating the triple products as repeated double products, as noted by Van Dyke and Guttmann [5]. For this purpose, we expand q^2 as

(2.5) $$q^2 = q_0^2 + \delta q_1^2 + \delta^2 q_2^2 + \delta^3 q_3^2 + \cdots.$$

The equations at the first few orders are given as

(2.6a) (i) $$\nabla^2\phi_0 = 0,$$

(2.6b) $$q_0^2 = \nabla\phi_0 \cdot \nabla\phi_0,$$

(2.7a) (ii) $$\nabla^2\phi_1 = [1/(\gamma-1)]\nabla\phi_0 \cdot \nabla q_0^2,$$

(2.7b) $$q_1^2 = 2\nabla\phi_1 \cdot \nabla\phi_0,$$

(2.8a) (iii) $$\nabla^2\phi_2 = q_0^2\nabla^2\phi_1 + [1/(\gamma-1)][\nabla\phi_0 \cdot \nabla q_1^2 + \nabla\phi_1 \cdot \nabla q_0^2],$$

(2.8b) $$q_2^2 = 2\nabla\phi_2 \cdot \nabla\phi_0 + \nabla\phi_1 \cdot \nabla\phi_1,$$

and so forth.

The boundary conditions at different orders are

(2.9a) $$\phi_0 + c\phi_{0y} = U \sin x \quad \text{on } y = 0,$$

(2.9b) $$\phi_n + c\phi_{ny} = 0 \quad \text{on } y = 0, \quad n = 1, 2, 3, \cdots,$$

(2.9c) $$\phi_n \to 0 \quad \text{as } y \to \infty, \quad n = 0, 1, 2, 3, \cdots.$$

The procedure can be continued and carried out order by order. The solution at the first few orders are found to be

(2.10a) $$\phi_0 = [1/(1-c)]\, e^{-y} \sin x,$$

(2.10b) $$\phi_1 = [-(5/8)(1-3c)/(1-c)^4]e^{-y} \sin x + [(5/8)/(1-c)^3]\, e^{-3y} \sin x,$$

(2.10c)
$$\begin{aligned}\phi_2 = {} & [(75/64)(1-3c)^2/(1-c)^7 - (65/32)(1-5c)/(1-c)^6]\, e^{-y} \sin x \\ & - [(75/64)(1-3c)/(1-c)^6]\, e^{-3y} \sin x \\ & + [(65/32)/(1-c)^5]\, e^{-5y} \sin x \\ & + [(25/128)(1-5c)/(1-3c)^6]\, e^{-3y} \sin 3x \\ & - [(25/128)/(1-c)^5]\, e^{-5y} \sin 3x\end{aligned}$$

and

$$q_0^2=[1/(1-c)^2]\,e^{-2y}, \tag{2.11a}$$

$$\begin{aligned} q_1^2=&[(-5/4)(1-3c)/(1-c)^5]\,e^{-2y}+[(5/2)(1-c)^4]\,e^{-4y}\\ &-[(5/4)/(1-c)^4]\,e^{-4y}\cos 2x, \end{aligned} \tag{2.11b}$$

$$\begin{aligned} q_2^2=&[(175/64)(1-3c)^2/(1-c)^8-(65/16)(1-5c)/(1-c)^7]\,e^{-2y}\\ &-[(25/4)(1-3c)/(1-c)^7]\,e^{-4y}+[(905/64)/(1-c)^6]\,e^{-6y}\\ &+[(75/64)(1-5c)/(1-3c)(1-c)^6\\ &\qquad+(25/8)(1-3c)/(1-c)^7]\,e^{-4y}\cos 2x\\ &-[(45/4)/(1-c)^6]\,e^{-6y}\cos 2x+[(25/64)/(1-c)^6]\,e^{-6y}\cos 4x. \end{aligned} \tag{2.11c}$$

We will address the singularities evident in (2.11) in § 3.

It has been checked that the maximum velocity occurs at $y=0$ and $x=\pi/2+2n\pi$, n an integer. For example, taking $c=0$ gives the maximum velocity to be

$$q_{\max}^2=1+(5/2)\delta+(890/64)\delta^2+\cdots. \tag{2.12}$$

Higher order terms beyond the first few are involved and the extension of the series has been relegated to a computer. The early terms of the series have been calculated with the help of the symbolic manipulation computer language Macsyma. This serves to reveal the form of the general term of the expansion. A Fortran program was then written to extend the series to arbitrary order. To check the accuracy of the computation, calculations have been done using double precision and then quadruple precision (32 significant figures). Up to 36 terms of the series were obtained on an IBM 3081. Comparison of the two calculations indicates an accuracy of at least 10 significant figures. Velocity series and velocity potential series have been obtained with different choices of c in the boundary condition and at different field points.

In the following section, the series are analyzed to find their singularities and hence their radii of convergence, $\delta_{\lim}$. In each case, the radius of convergence is compared with δ_{cr}, the value at which sonic speed is first attained. Equality of the two quantities is often taken to mean that smooth continuous flow does not exist beyond sonic conditions; as we pointed out in the Introduction this assertion is in general unwarranted.

3. Analysis of series. q^2-series are obtained with different choices of c in the boundary condition and at different field points. Sample results are shown in Tables 1 and 2.

Determination of δ_{cr}. First we determine the value of the perturbation parameter δ_{cr} for which the flow becomes locally sonic. Local sonic flow occurs first at $x=\pi/2+2n\pi$ and $y=0$, where the velocity is maximum. Putting $a^2=q_{\max}^2$ into the energy conservation equation (1.3), we get

$$q_{\max}^2[(\gamma+1)(\gamma-1)]=1/\delta, \tag{3.1}$$

and substituting the series $q_{\max}^2=\sum q_n^2\delta^n$ into (3.1), we obtain a sequence of polynomial equations in δ. *The smallest positive roots of the equations are found and checked to determine whether they exhibit a converging trend.* If n terms of the $q_{\max}^2$-series are used, then the root gives an estimate of δ_{cr} to the nth approximation.

To get the best estimate of the limit of the sequence of approximations to δ_{cr}, one can employ a nonlinear transformation to hasten the rate of convergence [24]. An

TABLE 1

Coefficients of $q^2_{\max}$-series evaluated at $x=\pi/2$, $y=0$ for different boundary conditions.

n	q^2_n $(c=-0.5)$	q^2_n $(c=0)$	q^2_n $(c=0.5)$	q^2_n $(c=1.5)$
0	0.444444E+00	1.000000E+00	4.000000E+00	4.000000E+00
1	0.329218E+00	0.250000E+01	0.800000E+02	−0.800000E+02
2	0.582228E+00	0.139063E+02	0.298000E+04	0.250571E+04
3	0.122283E+01	0.959440E+02	0.133312E+06	−0.926689E+05
4	0.284073E+01	0.742746E+03	0.664100E+07	0.375463E+07
5	0.705012E+01	0.617153E+04	0.354328E+09	−0.161416E+09
6	0.183397E+02	0.537905E+05	0.198108E+11	0.723260E+10
7	0.494234E+02	0.485270E+06	0.114567E+13	−0.334092E+12
8	0.136918E+03	0.449327E+07	0.679637E+14	0.157969E+14
9	0.387834E+03	0.424597E+08	0.411278E+16	−0.760833E+15
10	0.111895E+04	0.407842E+09	0.252892E+18	0.371963E+17
11	0.327872E+04	0.397040E+10	0.157555E+20	−0.184110E+19
12	0.973559E+04	0.390885E+11	0.992405E+21	0.920803E+20
13	0.292434E+05	0.388504E+12	0.630937E+23	−0.464623E+22
14	0.887352E+05	0.389307E+13	0.404345E+25	0.236238E+24
15	0.271687E+06	0.392888E+14	0.260935E+27	−0.120917E+26
16	0.838570E+06	0.398976E+15	0.169416E+29	0.622538E+27
17	0.260713E+07	0.407391E+16	0.110588E+31	−0.322176E+29
18	0.815925E+07	0.418021E+17	0.725338E+32	0.167505E+31
19	0.256894E+08	0.430812E+18	0.477786E+34	−0.874506E+32
20	0.813319E+08	0.445750E+19	0.315939E+36	0.458273E+34
21	0.258813E+09	0.462856E+20	0.209649E+38	−0.240969E+36
22	0.827494E+09	0.482183E+21	0.139561E+40	0.127098E+38
23	0.265740E+10	0.503811E+22	0.931744E+41	−0.672280E+39
24	0.856909E+10	0.527846E+23	0.623718E+43	0.356524E+41
25	0.277387E+11	0.554415E+24	0.418550E+45	−0.189526E+43
26	0.901176E+11	0.583672E+25	0.281508E+47	0.100974E+45
27	0.293775E+12	0.615793E+26	0.189735E+49	−0.539071E+46
28	0.960773E+12	0.650977E+27	0.128130E+51	0.288344E+48
29	0.315175E+13	0.689451E+28	0.866855E+52	−0.154507E+50
30	0.103691E+14	0.731465E+29	0.587461E+54	0.829296E+51
31	0.342078E+14	0.777299E+30	0.398751E+56	−0.445808E+53
32	0.113149E+15	0.827263E+31	0.271064E+58	0.240006E+55
33	0.375200E+15	0.881698E+32	0.184523E+60	−0.129388E+57
34	0.124714E+16	0.940980E+33	0.125778E+62	0.698438E+58
35	0.415491E+16	0.100552E+35	0.858412E+63	−0.377480E+60
36	0.138727E+17	0.107578E+36	0.586542E+65	0.204250E+62

effective method is the ε-algorithm of Barber et al. [25]. If $\{f_n\}$ denotes the sequence of approximations to $\delta_{\rm cr}$, this scheme of successive nonlinear transformations is defined as

$$f_n^{(m+1)}=f_n^{(m)}+1/[\varepsilon_n^{(m)}+\varepsilon_{n-1}^{(m)}], \tag{3.2a}$$

$$\varepsilon_n^{(m)}=a_m\varepsilon_n^{(m-1)}+1/[f_{n+1}^{(m)}+f_n^{(m)}] \tag{3.2b}$$

where $a_m=0$ if m is even and $a_m=-1$ if m is odd:

$$\{f_n^{(0)}\}=\{f_n\} \quad\text{and}\quad \varepsilon_n^{(-1)}=0, \qquad n=1,2,3,\cdots.$$

Table 3 lists the values of $\delta_{\rm cr}$ for various $q^2_{\max}$-series. The determination of the values is based on the apparent convergence in applying the ε-algorithm.

When $c>1$, the radius of convergence of the q^2-series is limited by the nearest singularity lying on the negative real axis of δ. Though this singularity is nonphysical,

TABLE 2
Coefficients of q^2-series evaluated at $x = \pi/4$, $y = 0$ for different boundary conditions.

n	q_n^2 $(c=-0.5)$	q_n^2 $(c=0)$	q_n^2 $(c=0.5)$	q_n^2 $(c=1.5)$
0	0.444444E+00	1.000000E+00	4.000000E+00	4.000000E+00
1	0.823045E−01	0.125000E+01	0.600000E+02	−0.100000E+03
2	0.127267E+00	0.617188E+01	0.223500E+04	0.327500E+04
3	0.130576E+00	0.343327E+02	0.101279E+06	−0.123394E+06
4	0.528379E−01	0.211576E+03	0.509839E+07	0.505749E+07
5	−0.192304E+00	0.139982E+04	0.274050E+09	−0.219021E+09
6	−0.765748E+00	0.973388E+04	0.154028E+11	0.986219E+10
7	−0.188091E+01	0.702369E+05	0.894161E+12	−0.457173E+12
8	−0.356724E+01	0.521748E+06	0.531972E+14	0.216741E+14
9	−0.470825E+01	0.396916E+07	0.322650E+16	−0.104607E+16
10	0.720851E−01	0.308117E+08	0.198757E+18	0.512261E+17
11	0.293821E+02	0.243449E+09	0.124015E+20	−0.253898E+19
12	0.139047E+03	0.195426E+10	0.782130E+21	0.127128E+21
13	0.482763E+03	0.159170E+11	0.497786E+23	−0.642085E+22
14	0.145891E+04	0.131406E+12	0.319309E+25	0.326738E+24
15	0.405347E+04	0.109881E+13	0.206225E+27	−0.167359E+26
16	0.106193E+05	0.930131E+13	0.133990E+29	0.862179E+27
17	0.266174E+05	0.796688E+14	0.875183E+30	−0.446441E+29
18	0.645063E+05	0.690239E+15	0.574348E+32	0.232226E+31
19	0.152656E+06	0.604700E+16	0.378518E+34	−0.121294E+33
20	0.357012E+06	0.535529E+17	0.250412E+36	0.635874E+34
21	0.838586E+06	0.479293E+18	0.166235E+38	−0.334474E+36
22	0.202121E+07	0.433370E+19	0.110702E+40	0.176475E+38
23	0.511972E+07	0.395742E+20	0.739333E+41	−0.933733E+39
24	0.138802E+08	0.364844E+21	0.495074E+43	0.495313E+41
25	0.404255E+08	0.339448E+22	0.332319E+45	−0.263371E+43
26	0.124941E+09	0.318592E+23	0.223571E+47	0.140350E+45
27	0.401604E+09	0.301510E+24	0.150724E+49	−0.749444E+46
28	0.131744E+10	0.287595E+25	0.101809E+51	0.400950E+48
29	0.435213E+10	0.276361E+26	0.688933E+52	−0.214886E+50
30	0.143653E+11	0.267418E+27	0.466979E+54	0.115357E+52
31	0.471980E+11	0.260452E+28	0.317032E+56	−0.620232E+53
32	0.154157E+12	0.255213E+29	0.215551E+58	0.333959E+55
33	0.500580E+12	0.251496E+30	0.146758E+60	−0.180064E+57
34	0.161733E+13	0.249138E+31	0.100052E+62	0.972119E+58
35	0.520506E+13	0.248009E+32	0.682938E+63	−0.525461E+60
36	0.167060E+14	0.248006E+33	0.466709E+65	0.284354E+62

TABLE 3
List of the values of δ_{cr} for various q^2_{max}-series.

c	−1.5	−0.5	−0.1	0	0.3	0.5	0.8
δ_{cr}	0.848301	0.261443	0.118695	0.089616	0.019714	0.014035	0.0009116

its presence limits the utility of the series expansion. We defer the discussion of this case to the end of this section.

Nonexistence of solutions for $c = 1, 1/3, 1/5, \cdots$. Examination of the terms in the potential expansion (2.10) shows that these diverge for $c = 1, 1/3, 1/5, \cdots, 1/(2n+1), \cdots$, for all integer n. *We conjecture the nonexistence of bounded solutions to our problem for all such values of c.* The basis for this conjecture is the following simple linear problem:

(3.3a) $$\nabla^2\phi = 0, \qquad y > 0,$$

(3.3b) $$\phi + c\phi_y = U \sin x, \qquad y = 0.$$

This problem has no bounded solution for $c = 1$. The proof of this is immediate, since if we assume that ϕ is bounded, we can easily construct the solution and from this find that the solution to (3.3) has a pole at $c = 1$. (Linear problems of this sort, for which no bounded solution exists have been treated in generality by Agmon, Douglas and Nirenberg [26].) As the construction of (2.10) demonstrates the nonlinear equation (2.3) generates the additional poles at $1/(2n+1)$ and thus our conjecture.

Singularity structure and the radius of convergence. The next step is to determine the location and the nature of the nearest singularity $\delta_{\lim}$ of each of the q^2-series.

(1) *Ratio method of Domb and Sykes* [12]. The convergence of the series in δ is limited by the singularity closest to the origin at $\delta_{\lim}$. We shall suppose the relation [27]

(3.4a) $$p(\delta) = \Sigma_0^\infty p_n \delta^n = (1 - \delta/\delta_{\lim})^{-\nu} b(\delta) + a(\delta)$$

with

(3.4b) $$b(\delta) = \Sigma_0^\infty b_n(\delta - \delta_{\lim})^n, \; a(\delta) = \Sigma_0^\infty a_n(\delta - \delta_{\lim})^n,$$

where the functions $b(\delta)$ and $a(\delta)$ have their respective radii of convergence greater than $\delta_{\lim}$. Then the ratio $r_n = p_n/p_{n-1}$ has the asymptotic expansion

(3.5) $$r_n \sim (1/\delta_{\lim})\{1 + (\nu-1)/n + (\nu-1)b_1\delta_{\lim}/[n(\nu+n-2)b_0] + O(1/n^3)\}.$$

To estimate $1/\delta_{\lim}$ from a finite number of terms of p_n, a natural method is to fit polynomials by Lagrangian interpolation in $(1/n)$ to r_n and extrapolating to $1/n = 0$. This can be accomplished by constructing a Neville table [13]. The sequence of jth-order extrapolants in the Neville table is given as [13]

(3.6) $$L_n^{(j)} = [nL_n^{(j-1)} - (n-j)L_{n-1}^{(j-1)}]/j$$

with

$$L_n^{(0)} = r_n, \qquad n = 1, 2, 3, \cdots.$$

The estimate of $1/\delta_{\lim}$ can be read off from the value to which the entries in the Neville table are apparently converging.

To estimate ν, the critical exponent, one can form the sequence $\{\nu_n\}$

(3.7) $$\nu_n = nr_n\bar{\delta}_{\lim} - n + 1$$

where $\bar{\delta}_{\lim}$ is the best estimate of $\delta_{\lim}$ from the Neville table. The sequence $\{\nu_n\}$ can then be extrapolated to $1/n = 0$ by any sequence transformation to obtain the best estimate of ν.

Examination of the coefficients of the q^2-series in Tables 1 and 2 shows that the signs are either fixed or alternating. This suggests that the nearest singularities will probably be of algebraic type, the usual kind in most solution of physical problems. Neville tables are constructed to find the location of nearest singularity for different q^2-series.

(2) *Method of Padé approximants* [14]–[20]. The other widely used method for identifying singularities of a power series is Padé approximants. For a typical series of the form

(3.8) $$p(\delta) = p_0 + p_1\delta + p_2\delta^2 + \cdots + p_{m+n}\delta^{m+n} + \cdots$$

the $[m/n]$ Padé approximants to $p(\delta)$ is the rational polynomial expression

$$R_m(\delta)/S_n(\delta)=(r_0+r_1\delta+\cdots+r_m\delta^m)/(1+s_1\delta+\cdots+s_n\delta^n) \tag{3.9}$$

where the coefficients $r_0,\cdots,r_m$, $s_1,\cdots,s_n$ are uniquely determined so as to make the first $m+n+1$ terms of the expansion of (3.9) agree with the corresponding terms in (3.8) of $p(\delta)$. A table of Padé approximants $[m/n]$ can be constructed with varying m and n but $m+n$ cannot be greater than the total number of terms in the q^2-series.

Since the Padé approximants will represent all singularities as poles, it therefore will be most accurate if the singularity is a pole. As suggested by Baker [16], it is advisable to find the Padé approximants to the logarithmic derivative of the function. For example, for $p(\delta)$ as defined by (3.4a) we have

$$d[\log p(\delta)]/d\delta \sim -\nu/(\delta-\delta_{\lim}). \tag{3.10}$$

The pole closest to the origin of the Padé approximants is located by the smallest root of the denominator polynomial $S_n(x)$.

To find ν, Baker [16] proposed forming the Padé approximants to

$$(\delta_{\lim}-\delta)d[\log p(\delta)]/d\delta \sim -\nu \tag{3.11}$$

for an assumed value of $\delta_{\lim}$ and then to obtain an estimate of ν by evaluating the Padé approximants at $\delta=\delta_{\lim}$. Padé approximants to the $q^2_{\max}$-series and to the logarithmic derivative of the $q^2_{\max}$-series are used as alternative methods to locate the nearest singularities of the series. In general the converging trends in Padé tables are less apparent than those in Neville tables.

First the radius of convergence is found for each of the $q^2_{\max}$-series. When $c\geqq 0$, the entries in Neville tables show marked converging trends indicating that the nearest singularities $\delta_{\lim}$ are algebraic. As an example, the Neville table for $c=0$ is shown in Table 4. One can confirm from the converging trend of the data that $\delta_{\lim}=0.089616$ (accuracy to sixth decimal place) for $c=0$. Values of $\delta_{\lim}$ are read off from the tables and then used to find the critical exponent ν. Padé approximants to the series and to the logarithmic derivative of the series are also calculated to check the estimates for $\delta_{\lim}$. The agreement between estimates using different methods are very good to excellent. Domb-Sykes plots for $c=0.5$ and $c=0$, Figs. 1a and 1b, are good straight lines and are representative of the case $c\geqq 0$.

However for $c<0$, both the Neville tables and Padé tables fail to exhibit converging trends. As we see in Fig. 1c, the Domb-Sykes plot for $c=-0.5$ shows a nonzero curvature. This suggests that the closest singularity for $c=-0.5$ is not of algebraic type or algebraic but not on real axis. Another resort is to apply the ε-algorithm to the sequence $\{r_n\}$, where r_n is the ratio of consecutive coefficients. This technique was used by Van Dyke and Guttmann [5] in their estimation of the radius of convergence of the velocity series for compressible flow over a circle. It has been used successfully here to find estimates for $\delta_{\lim}$. Such a method will be successful if the ratios of successive coefficients appear as $r_n\sim(1/\delta_{\lim})(1-a/n^a)$. However, the nature of singularity structure suggested by such behavior is still not known.

(i) $0\leqq c<1$. Table 5 locates the nearest singularity $\delta_{\lim}$ and critical exponent ν for various values of c in this range. Comparison of this table with Table 3 indicates that within numerical tolerance $\delta_{\lim}=\delta_{\mathrm{cr}}$. Thus the series solution (2.11) ceases to converge beyond the critical value. Although nothing definite can be said about the smoothness of flows for $\delta>\delta_{\lim}=\delta_{\mathrm{cr}}$, it is perhaps likely that shocks do occur then since the singularity is on the positive real axis.

(ii) $c<0$. Table 6 locates the nearest singularity $\delta_{\lim}$ for various values of c less than 0. As mentioned above, the nature of the nearest singularity is not of algebraic

TABLE 4

Neville table of the $q^2_{\max}$-series for $c = 0$. Only the first and last few columns are shown.

$1/r_n$	$1/L_n^{(2)}$	$1/L_n^{(4)}$	$1/L_n^{(6)}$	$1/L_n^{(8)}$
0.40000000				
0.17977528				
0.14494130	0.09953170			
0.12917471	0.09121986			
0.12035047	0.09052134	0.09039570		
0.11473263	0.09015929	0.08966996		
0.11084648	0.08995452	0.08959526	0.08957195	
0.10799940	0.08983403	0.08958498	0.08958327	
0.10582421	0.08976123	0.08959356	0.08961123	0.08962352
0.10410839	0.08971577	0.08960070	0.08961279	0.08961202
0.10272045	0.08968629	0.08960414	0.08960864	0.08960357
0.10157467	0.08966649	0.08960581	0.08960803	0.08960825
0.10061282	0.08965277	0.08960691	0.08960925	0.08961199
0.09979393	0.08964302	0.08960781	0.08961048	0.08961278
0.09908836	0.08963594	0.08960860	0.08961131	0.08961274
0.09847412	0.08963071	0.08960929	0.08961186	0.08961286
0.09793457	0.08962678	0.08960989	0.08961226	0.08961316
0.09745688	0.08962380	0.08961041	0.08961260	0.08961348
0.09703100	0.08962152	0.08961086	0.08961289	0.08961375
0.09664893	0.08961974	0.08961125	0.08961314	0.08961396
0.09630424	0.08961836	0.08961159	0.08961337	0.08961413
0.09599172	0.08961727	0.08961189	0.08961356	0.08961428
0.09570706	0.08961642	0.08961217	0.08961374	0.08961441
0.09544670	0.08961574	0.08961241	0.08961389	0.08961453
0.09520766	0.08961520	0.08961262	0.08961403	0.08961463
0.09498742	0.08961477	0.08961282	0.08961415	0.08961473
0.09478384	0.08961443	0.08961300	0.08961426	0.08961481
0.09459512	0.08961416	0.08961316	0.08961437	0.08961489
0.09441967	0.08961395	0.08961331	0.08961446	0.08961496
0.09425616	0.08961379	0.08961345	0.08961454	0.08961502
0.09410339	0.08961366	0.08961357	0.08961462	0.08961508
0.09396035	0.08961356	0.08961369	0.08961469	0.08961513
0.09382614	0.08961349	0.08961379	0.08961476	0.08961518
0.09369996	0.08961343	0.08961389	0.08961482	0.08961523
0.09358111	0.08961340	0.08961398	0.08961488	0.08961527
0.09346898	0.08961337	0.08961407	0.08961493	0.08961531

$1/L_n^{(27)}$	$1/L_n^{(29)}$	$1/L_n^{(31)}$	$1/L_n^{(33)}$	$1/L_n^{(35)}$
0.08961572				
0.08961575				
0.08961578	0.08961579			
0.08961582	0.08961583			
0108961586	0.08961586	0.08961587		
0.08961588	0.08961589	0.08961589		
0.08961590	0.08961591	0.08961592	0.08961592	
0.08961592	0.08961593	0.08961594	0.08961595	
0.08961594	0.08961595	0.08961596	0.08961597	0.08961597

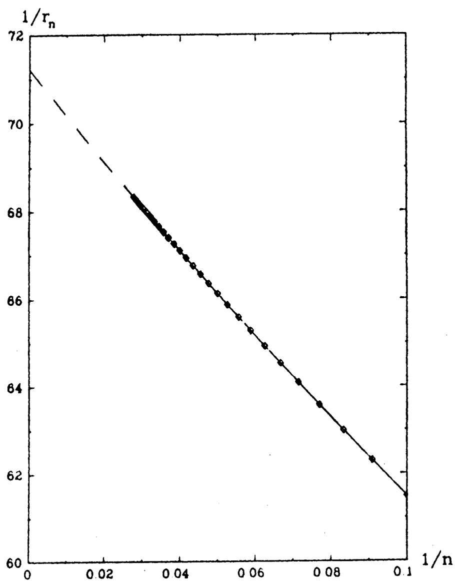

FIG. 1a. *Domb-Sykes plot for* $c = 0.5$.

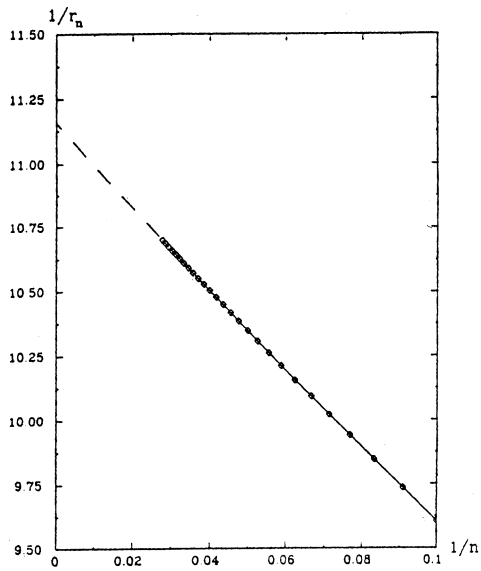

FIG. 1b. *Domb-Sykes plot for* $c = 0$.

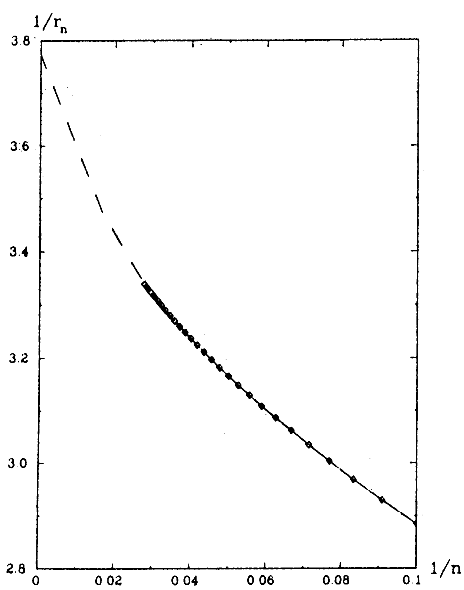

FIG. 1c. *Domb-Sykes plot for* $c = -0.5$.

type and therefore the critical exponent is not applicable in this range. Comparison of Table 6 with Table 3 shows that $\delta_{\text{lim}} > \delta_{\text{cr}}$ by 1 to 3 percent on average. Hence the series solution converges beyond $\delta = \delta_{\text{cr}}$ and smooth flows persist beyond sonic conditions.

TABLE 5
List of the values of δ_{lim} for various q^2_{max}-series $(0 \leqq c < 1)$.

c	0	0.3	0.5	0.8
δ_{lim}	0.089616	0.019717	0.014041	0.0009118
ν	−0.514	−0.508	−0.505	−0.503

TABLE 6
List of the values of δ_{lim} for various q^2_{max}-series $(c < 0)$.

c	−1.5	−0.5	−0.1
δ_{lim}	0.88	0.265	0.1206

The case $c > 1$ will be discussed separately later in this section.

Figure 2 shows the plot of q^2_{max} against δ for two different cases. The plot exemplifies the divergence of the q^2_{max}-series beyond their respective radii of convergence. For $c > 1$ the singularity lies on the negative axis while for $c < 1$ it is on the positive axis.

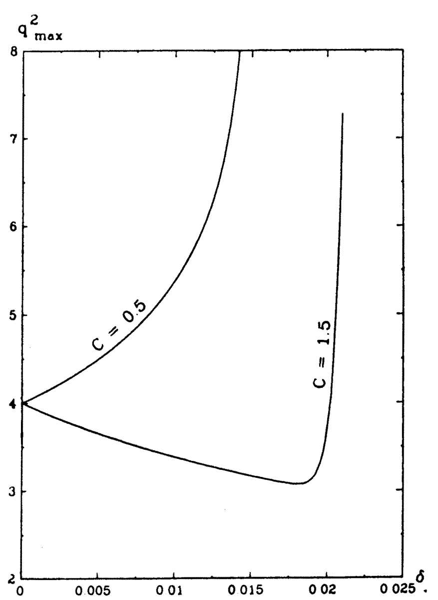

FIG. 2. *Plot of q^2_{max} against δ for $c = 1.5$ and $c = 0.5$.*

It is instructive to find the maximum local Mach number given by

$$M^2 = q_{\max}^2 / a^2 \tag{3.12}$$

where a^2 can be obtained from (1.3) as

$$a^2 = [(\gamma - 1)/2][1/\delta - q_{\max}^2]. \tag{3.13}$$

Hence

$$M^2 = [2/(\gamma - 1)]\delta q_{\max}^2 / (1 - \delta q_{\max}^2), \tag{3.14}$$

which can be easily computed using the $q_{\max}^2$-series. Graphs of M^2 against δ for different cases are shown in Fig. 3. We observe that the plot diverges well below sonic conditions for $c = 1.5$ and diverges approximately at sonic conditions for $0 \leqq c < 1$.

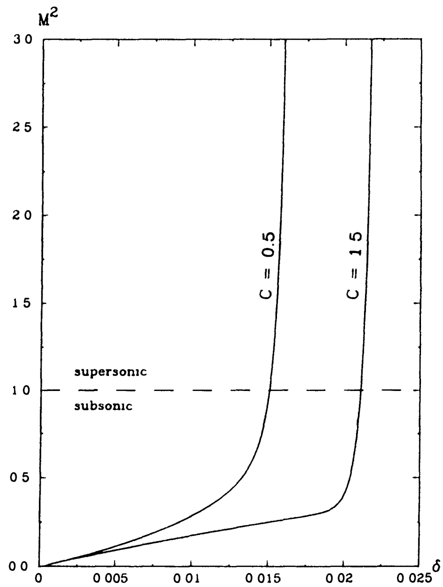

FIG. 3. *Plot of M^2 against δ for $c = 1.5$ and $c = 0.5$.*

We also plot the isobars of the flow fields for $c = 1.5$ and $c = 0$ at values of δ which are close to the limits of convergence in Figs. 4a and 4b. The values of the isobars are normalised with respect to the minimum pressure at $x = \pi/2$, $y = 0$.

The radius of convergence was also found for the q^2-series evaluated at other field points such as $x = \pi/4$, $y = 0$ and $x = \pi/8$, $y = 0$. For $c > 0$, we find that the estimates of $\delta_{\lim}$ are independent of the field point at which the series is evaluated. However, for $c < 0$ and $c = 0$, the nearest singularity of q^2-series other than $q_{\max}^2$ cannot be located as all the above methods fail to give any reasonable sense of convergence. Following a method of Hunter and Guerrieri [27] we also tested for conjugate pairs of complex algebraic singularities, but these attempts were unsuccessful.

$c > 1$, *a convergent example.* The case $c > 1$ is of special interest and will be treated now in some detail. In Table 7 we give results of the sort given previously. We first

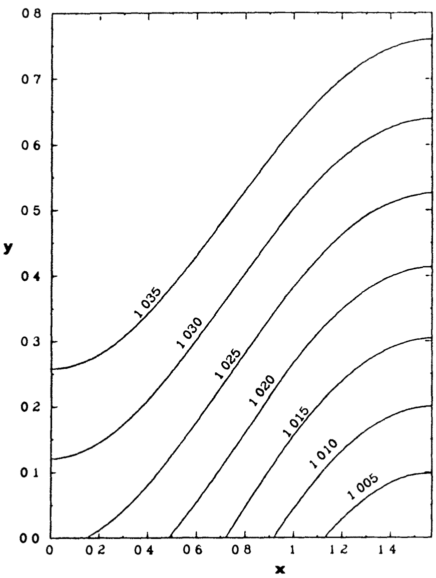

FIG. 4a. *Plot of isobars for* $c = 1.5$ *and* $\delta = 0.0175$.

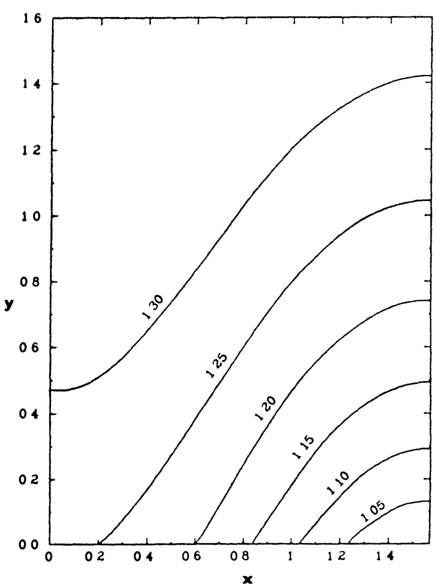

FIG. 4b. *Plot of isobars for* $c = 0$ *and* $\delta = 0.089$.

note that the singularity, which is of square root type, lies on the negative real axis and is therefore unphysical. Also we see that δ_{lim} can be quite small in magnitude. In fact convergence of the series (2.10), (2.11) is now restricted to values of δ well below δ_{cr}, i.e., convergence fails before sonic conditions are achieved (see Fig. 3). On the other

TABLE 7
List of the values of δ_{lim} for various q^2_{max}-series ($c > 1$).

c	1.1	1.3	1.5	1.7
δ_{lim}	−0.000121574	−0.00350274	−0.0177376	−0.0556437
ν	−0.500	−0.500	−0.500	−0.500

hand since the singularity is on the negative real axis we can hope to transform it away. We therefore attempt to use the Euler transformation to map δ_{lim} to infinity. This is accomplished by recasting the series in the new perturbation parameter $e = \delta/(\delta - \delta_{\text{lim}})$. The radius of convergence is then extended to some further singularity. The nearest singularity of the transformed series was then investigated by Padé approximants and the radius of convergence found to be greater than 1. This implies that the original series does not have a singularity in the right half plane $\text{Re}\,\delta > \delta_{\text{lim}}$. Therefore we have constructed a flow field which goes smoothly from subsonic into supersonic condition without shocks.

As a verification another useful method for the analytic continuation of the series is the use of Padé approximants. This is due to the property that Padé approximants is invariant under Euler transformation [15]. In fact, if $R_m(x)/S_m(x)$ is the $[m/m]$ Padé approximants to $p(x)$, then $R_m(Ay/(1+By))/S_m(Ay/(1+By))$ is the $[m/m]$ Padé approximants to $p(Ay/(1+By))$. Using the information that q^2 is finite for infinite δ, the Padé approximants are found with numerator and denominator having the same degree.

Values of q^2_{max} and M^2 were calculated up to relatively large values of δ using the Euler transformed series and Padé approximants. The agreement of the two methods was excellent. Results of these calculations are plotted in Fig. 5 and Fig. 6, respectively.

Additional comments. We also repeated the series analysis described above using the velocity potential instead of q^2. The results were the same except in the case $c = 0$. When $c = 0$, $\phi = U \sin x$ at $y = 0$ and the ϕ expansion is reduced to a single term.

For each of the cases in which the critical exponent could be identified the nature of the singularity appears to be close to a square root branch point. Since this implies a double valuedness in the neighborhood of δ_{lim} a likely course to pursue is inversion of the q^2_{max}-series. These inverted series were investigated to find the nature and location of the nearest singularity but the Neville tables do not exhibit marked converging trends. Also the Padé tables gave estimates of the nearest singularity of the inverted series which were close to that of the original series. In this sense the reversion procedure provides no further information about the nature of the series.

In the study by Bollmann [10] of subsonic flow along a sinusoidal wall in the transonic approximation he reported that the series expansion of the u_{max} was a Stieltjes series, with the result that the series failed to converge beyond the critical Mach number. The point is that exponentially small terms contributed. We therefore applied the test for Stieltjes series to our case but found that the basic moment property failed, so Bollmann's procedure could not be applied.

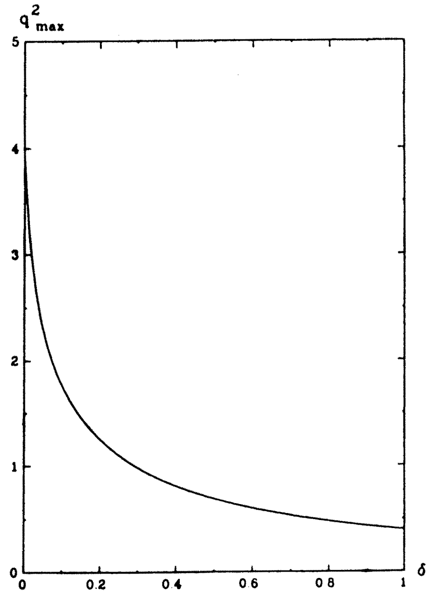

FIG. 5. *Plot of* $q_{\max}^2$ *against* δ *using Euler transform series and Padé approximants for* $c = 1.5$.

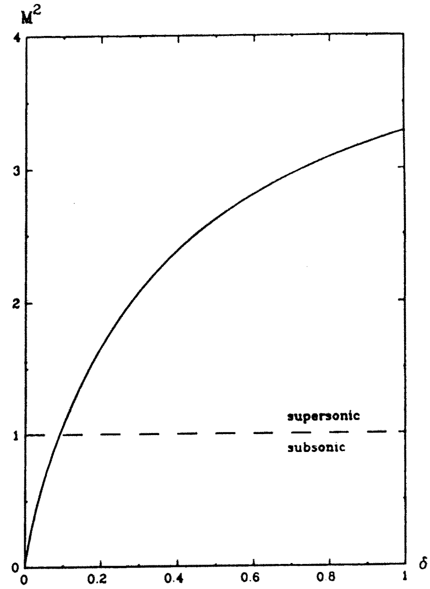

FIG. 6. *Plot of* M^2 *against* δ *using Euler transform series and Padé approximants for* $c = 1.5$.

4. Conclusions. Our calculations offer a solution to the compressible potential equation as a regular perturbation series and furnishes another example of extension of perturbation series by a computer. The primary conclusion is that the phenomenon of shockless transonic flow is dependent on the imposed boundary condition. Van Dyke and Guttmann [5] and Bollmann [10] considered different flow configurations and have reached apparently contradictory conclusions about the appearance of shocks in transonic flow. Here by varying the boundary condition we have shown that there is a continuous range of boundary conditions where $\delta_{\lim}$ is higher than δ_{cr} by a few percent. This implies the existence of smooth transonic solution. On the other hand another range of boundary condition gives $\delta_{\lim} = \delta_{cr}$ suggesting that shocks will commence at sonic condition. Also we have constructed a flow field that is smooth for all Mach numbers.

For $c > 0$, the location and nature of singularity do not change with the field point. Within this range of c, the problem remains elliptic in its circle of convergence since $\delta_{\lim} = \delta_{cr}$. For $c < 0$, the singularity structure does change with the field point and, in this case, the flow is mixed elliptic-hyperbolic in its circle of convergence. For the bounding case, $c = 0$, the problem is elliptic in its circle of convergence but the singularity structure changes with field point. It is worthwhile to mention Whitley's [28] work on the regular perturbation series solution of potential flow past a sinusoidal wall of finite amplitude. His problem is elliptic, but the choice of field point does affect the behavior of convergence of the power series.

It is interesting, and perhaps disquieting, to observe that at successive orders only the Poisson equation is solved, even though in a number of cases the problem is mixed elliptic-hyperbolic. Thus we have constructed continuous solutions beyond sonic conditions using only elliptic operators.

REFERENCES

[1] G. I. TAYLOR, *Recent work on the flow of compressible fluids*, J. London Math. Soc., 5 (1930), pp. 224-240.

[2] L. BERS, *Mathematical Aspects of Subsonic and Transonic Gas Dynamics*, John Wiley, New York, 1958.

[3] M. J. LIGHTHILL, *Higher approximation*, in General Theory of High Speed Aerodynamics, W. R. Sears, ed., Section E, Princeton Univ. Press, 1954, pp. 345-489.

[4] C. S. MORAWETZ, *On the nonexistence of continuous transonic flow past profiles* II, Comm. Pure Appl. Math., 10 (1957), pp. 107-131.

[5] M. D. VAN DYKE AND A. J. GUTTMANN, *Subsonic potential flow past a circle and the transonic controversy*, J. Austral. Math. Soc. Ser. B, 24 (1983), pp. 243-261.

[6] H. GÖRTLER, *Gas flows with transition from subsonic to supersonic velocities*, Z. Angew. Math. Mech., 20 (1940), pp. 254-273.

[7] I. IMAI AND S. OYAMA, *Application of thin wing expansion method to gas flow along sinusoidal wall*, Rep. Inst. of Sci. & Tech., Univ. of Tokyo, 2 (1948), pp. 39-44.

[8] C. KAPLAN, *On a solution of the non-linear differential equation for transonic flow past a wave-shaped wall*, NACA Tech Note 2383, 1952.

[9] ———, *On transonic flow past a wave-shaped wall*, NACA Tech Note 2748, 1953.

[10] G. BOLLMANN, *Potential flow along a wavy wall and transonic controversy*, J. Engrg. Math., 16 (1982), pp. 197-207.

[11] R. COURANT AND D. HILBERT, *Methods of Mathematical Physics*, Vol. II, Wiley-Interscience, New York, 1962.

[12] C. DOMB AND M. F. SYKES, *On the susceptibility of a ferromagnetic above the Curie point*, Proc. Roy. Soc. London Ser. A, 240 (1957), pp. 214-228.

[13] D. L. HUNTER AND G. A. BAKER, JR., *Methods of series analysis* I. *Comparison of current method used in the theory of critical phenomena*, Phys. Rev. B, 7 (1973), pp. 3346-3376.

[14] L. WUYTACK, ed., *Padé approximation and its applications*, Proceedings, Antwerp, Lecture Notes in Mathematics, Springer-Verlag, Berlin-Heidelberg-New York, 1979.

[15] G. A. BAKER, JR., *Essentials of Padé Approximants*, Academic Press, New York, 1975.

[16] ———, *Padé approximants, part* 1: *basic theory*, Encyclopedia of Mathematics and Its Applications, Addison-Wesley, Reading, MA, 1981.

[17] P. R. GRAVES-MORRIS, *Padé Approximants and Their Applications*, Academic Press, New York, 1972.

[18] H. CABANNES, ed., *Padé approximants method and its applications to mechanics*, Lecture Notes in Physics, Springer-Verlag, Berlin, New York, 1976.

[19] E. B. SAFF AND R. S. VARGA, eds., *Padé and Rational Approximation*: *Theory and Applications*, Academic Press, New York, 1976.

[20] G. A. BAKER, JR. AND J. L. GAMMEL, eds., *The Padé approximant in theoretical physics*, Mathematics in Science and Engineering, Vol. 71, Academic Press, New York, 1970.

[21] M. D. VAN DYKE, *Computer-extended series*, Ann. Rev. Fluid Mech., 16 (1983), pp. 287-309.
[22] ———, *Analysis and improvement of perturbation series*, Quart. J. Mech. Appl. Math., 27 (1974), pp. 423-450.
[23] ———, *Computer extension of perturbation series in fluid mechanics*, this Journal, 28 (1975), pp. 720-734.
[24] D. SHANK, *Nonlinear transformation of divergent and slowly convergent sequences*, J. Math. Phys., 34 (1955), pp. 1-42.
[25] M. N. BARBER AND C. J. HAMER, *Extrapolation of sequences using a generalized epsilon algorithm*, J. Austral. Math. Soc. Ser. B, 23 (1982), pp. 229-240.
[26] S. AGMON, G. DOUGLAS AND L. NIRENBERG, *Properties of solutions in Banach spaces*, Comm. Pure Appl. Math., 12 (1959), pp. 623-727.
[27] C. HUNTER AND B. GUERRIERI, *Deducing the properties of singularities of functions from their Taylor series coefficients*, this Journal, 39 (1980), pp. 248-263.
[28] N. L. WHITLEY, *Potential flow past a sinusoidal wall of finite amplitude*, J. Engrg. Math., 18 (1984), pp. 207-217.